Transcriptomic analyses reveal molecular mechanisms underlying regulation of floral attributes in Lonicera japonica Thunb.

Lei Shi
School of Basic Medical Sciences, Xinxiang Medical University, Xinxiang, 453003
Yuan Shen (s.y0001@163.com)
School of Pharmacy, Xinxiang Medical University, Xinxiang, 453003
Yuhao Chi
School of Pharmacy, Xinxiang Medical University, Xinxiang, 453003

Research Article

Keywords: Lonicera japonica, de novo transcriptome, flowering time, floral scent, flower color

Posted Date: March 2nd, 2021

DOI: https://doi.org/10.21203/rs.3.rs-216108/v1

Abstract

Background

Lonicera Japonica Thunb. is a perennial, semi-evergreen and twining vine in the family of Caprifoliaceae, which is widely cultivated in Asia. Thus far, *L. japonica* is often used to treat some human diseases including COVID-19, H1N1 influenza and hand-foot-and-mouth diseases, however, the regulatory mechanism of intrinsic physiological processes during different floral developmental stages of *L. japonica* remain largely unknown.

Results

The complete transcriptome of *L. japonica* was de novo-assembled and annotated, generating a total of 195850 unigenes, of which 84657 could be functionally annotated. 70 candidate genes involved in flowering transition were identified and the flowering regulatory network of five pathways was constructed in *L. japonica*. The mRNA transcripts of *AGL24* and *SOC1* exhibited a downward trend during flowering transition and followed by a gradual increase during the flower development. The transcripts of *AP1* was only detected during the floral development, whereas the transcript level of *FLC* was high during the vegetative stages. The expression profiles of *AGL24*, *SOC1*, *AP1* and *FLC* genes indicate that these key integrators might play the essential and evolutionarily conserved roles in control of flowering switch across the plant kingdom. We also identified 54 *L. japonica* genes encoding enzymes involved in terpenoid biosynthesis pathway. Most highly expressed genes centered on the MEP pathway, suggesting that this plastid pathway might represent the major pathway for terpenoid biosynthesis in *L. japonica*. In addition, 33 and 31 key genes encoding enzymes involved in the carotenogenesis and anthocyanin biosynthesis pathway were identified, respectively. *PSY* transcripts gradually increased during the flower development, supporting its role as the first rate-limiting enzyme in carotenoid skeleton production. The expression level of most anthocyanin biosynthetic genes was dramatically decreased during the flower developmental stages, consistent with the decline in the contents of anthocyanin.

Conclusion

These results identified a large number of potential key regulators controlling flowering time, flower color and floral scent formation in *L. japonica*, which improves our understanding of the molecular mechanisms underlying the flower traits and flower metabolism, as well as sets the groundwork for quality improvement and molecular breeding of *L. japonica*.

Introduction

Lonicera japonica Thunb. is a perennial, semi-evergreen and twining vine in the family of Caprifoliaceae. Since it has double-tongued flowers that open white and fade to yellow, this ornamental plant is also

called “Jin Yin Hua” in Chinese (literally “gold and silver flower”). *L. japonica* is widely cultivated in Asian countries such as China, Japan, and Korea. However, due to its strong viability, *L. japonica* is believed to be invasive to the ecology of some western counties [1]. *L. japonica* has been used as traditional Chinese Medicine for over thousands of years for its anti-bacterial, anti-viral, anti-endotoxin, anti-inflammatory and anti-pyretic properties and has been recorded in the “Shen Nong Ben Cao Jing” and “Ben Cao Gang Mu” (Compendium of Materia Medica) as early as the 17th century [2]. The commercial value of *L. japonica* in the herbal medicine trading market has increased rapidly in recent years. More than 30% of current traditional Chinese medicine prescriptions have been reported to contain extracts from different parts of *L. japonica* [3]. Thus far, *L. japonica* is often used to treat some human diseases such as acute respiratory syndromes, H1N1 influenza, hand-foot-and-mouth diseases, pancreatic cancer [4, 5]. In the current, a pandemic of coronavirus disease 2019 (COVID-19) has spread globally. COVID-19 is caused by severe acute respiratory syndrome coronavirus 2 (SARS-CoV-2). Recently, emerging data indicate that *L. japonica*-based substances may be effective in the prevention and treatment of SARS-CoV-2 infection [6–9]. Chlorogenic acid (CGA) and luteoloside are the main active components used for evaluating the quality of *L. japonica*. The contents of CGA and luteoloside are highest accumulation in alabastrum, while lower in other developmental stages [10, 11]. Although some transcriptomic studies have been conducted to analyze the biosynthesis of pharmaceutically active ingredients during the flower development [10–12], the regulatory mechanism of intrinsic physiological processes during different floral developmental stages of *L. japonica* remain largely unknown.

Flowering is an intricate biological process during the angiosperm life cycle. In recent years, the molecular framework for integrating different signaling pathways relevance to floral traits including flowering time, floral color and floral aroma have been studied in plants such as rice, gourds, potato and sorghum, poplar, citrus, and especially in model plant *Arabidopsis thaliana* [13, 14]. Flowering time are controlled by five major pathways, including the photoperiod pathway, the autonomous pathway, the vernalization pathway, the gibberellin pathway and the circadian clock pathway [15, 16]. More than 300 flowering genes have been established a comprehensive network to respond to endogenous or external environmental cues in *Arabidopsis* [15]. These genes activate or repress floral transformation through a small number of flower integrator genes, such as *FLOWERING LOCUS T* (*FT*), *FLOWERING LOCUS C* (*FLC*), *SUPPRESSOR OF OVEREXPRESSION OF CONSTANS 1* (*SOC1*), *AGAMOUS-LIKE 24* (*AGL24*), *APETALA1* (*AP1*) genes [17, 18]. Although the molecular aspect of flowering time control in *Arabidopsis* has been widely studied, the genes associated with *L. japonica* flowering time are almost unknown.

L. japonica also has commercial value for its fragrant volatiles that are widely used in manufacture of perfumes, scented oils, bathing products, and other household products. Terpenes with relative low molecular weight (such as monoterpenes and sesquiterpenes) account for the largest proportion of volatile organic compounds in *L. japonica* flowers [19]. The biosynthesis of plant volatile terpenes involves three steps: (1) production of the universal C5 isoprenoid precursors, isopentenyl diphosphate (IPP) and dimethylallyl diphosphate (DMAPP), (2) formation of geranyl diphosphate (GPP, C10) and farnesyl diphosphate (FPP, C15) by condensation of IPP with DMAPP, and (3) conversion of GPP and FPP substrates into monoterpenes and sesquiterpenes respectively. In the cytosol, IPP and DMAPP are derived

from acetyl-CoA through the mevalonic acid (MVA) pathway and catalyzed to FPP by farnesyl diphosphate synthase (FPPS). Then FPP is converted to the various sesquiterpenes by the cytosolic/mitochondrial terpene synthases (TPSs) [20]. In the plastids, IPP and DMAPP are synthesized from pyruvate and glyceraldehyde-3-phosphate (G3P) by the 2-C-methyl-D-erythritol 4-phosphate (MEP) pathway and converted into GPP by GPP synthase (GPPS). The plastidial TPSs catalyze GPP into the various monoterpenes [20]. The monoterpenes and sesquiterpenes may then be utilized to synthesize various terpene derivatives by cytochrome P450 (CYP450) enzymes, dehydrogenases and reductases, dehydrogenases and reductases [21]. For example, CYP76C1 and CYP76C3 catalyze linalool to 8-hydroxylinalool in *Arabidopsis* [22].

Flower color is directly determined by distinct colorful pigments. During *L. japonica* development, the flower color transits from the initial pale green to white and finally yellow. The developmental color change is mainly due to the increased contents of carotenoid as well as the decreased contents of chlorophyll and anthocyanin [23, 24]. The main pathways of anthocyanin and carotenoid biosynthesis have been well understood in model plants, and it is known to be fairly well conserved among the plants [25, 26]. Phytoene synthase (PSY) is the rate-limiting enzyme in carotenoid skeleton production. Phytoene then undergoes transformation catalyzed by phytoene desaturase (PDS), 15-cis-ζ-carotene isomerase (Z-ISO), ζ-carotene desaturase (ZDS), and carotenoid isomerase (CRTISO) to produce lycopene. Lycopene is transformed to δ-carotene and γ-carotene by lycopene ε-cyclase (LYCE) and lycopene β−cyclase (LYCB), respectively. Anthocyanin is one kind of water soluble natural pigment which belongs to flavonoid family. In the anthocyanin biosynthesis pathway, chalcone synthase (CHS), chalcone isomerase (CHI), flavanone 3-hydroxylase (F3H), Dihydroflavonol 4-reductase (DFR), anthocyanidin synthase (ANS), and UDP-glucose:flavonoid 3-O-glucosyltrasferase (UFGT) catalyze the sequential steps that are required for the synthesis of anthocyanin. Considering the intriguing color change during individual *L. japonica* flower development, it is interesting to study the molecular mechanisms of variation in *L. japonica* flower pigmentation.

The previous study of *L. japonica* mainly focused on the biosynthesis of pharmaceutically active ingredients [10–12, 27, 28], yet relevant researches for exploring the physiological and developmental regulation during *L. japonica* flower growth remain scarce. Here, we used RNA-seq technology to analyze the transcriptome of *L. japonica* leaf, flower bud, white flower and yellow flower tissues. Our detailed analysis identified a large number of potential key regulators controlling flowering time, flower color and floral scent formation. The expression patterns of the genes related to floral traits were analyzed and their dynamic regulatory networks were constructed in *L. japonica*. The results of this study improve our understanding of the molecular mechanisms underlying the flower traits and flower metabolism in *L. japonica*, as well as set the groundwork for quality improvement and molecular breeding of this species.

Methods

Plant materials

The fresh leaves, buds, white and yellow flowers were collected 5-year-old *L. japonica* plants from Fengqiu cultivation base (35°05'N and 114°25'E), Henan province, China. Samples with similar morphology (i.e., young leaves ~2 cm width, buds not yet bloomed into a full-size flower, white flowers and yellow flowers) were manually collected separately from three plants excluding subtending bract and bracteole. Samples of 3 plants at the same stage were combined and regarded as one biological replicate that representing each stage, and three independent replicates were performed. These samples were immediately frozen in liquid nitrogen following collection and stored at -80°C.

RNA extraction, cDNA library construction and transcriptome sequencing

Each sample was grounded to powder in liquid nitrogen using a mortar and pestle. Total RNA was extracted by using RNeasy Plant Mini kit (Qiagen, Hilden, Germany). The quantity and quality were determined using Agilent 2100 Bioanalyzer (Agilent Technologies, Santa Clara, CA, USA). The poly (A) mRNA was isolated from total RNA samples with Magnetic Oligo (dT) Beads (Illumina, San Diego, CA, USA) and mRNAs were added with fragmentation buffer to shear mRNA into short fragments (200 ~nt). First strand cDNA was synthesized using random hexamer primer and M-MuLV Reverse Transcriptase (RNase, H-), then second strand cDNA was synthesized using DNA polymerase I and RNase H. The AMPure XP system (Beckman Coulter, Beverly, USA) was used to select cDNA fragments preferentially 150-200 bp in length. Products were purified using AMPure XP system. The twelve libraries were sequenced using Illumina Hiseq X Ten platform.

De novo assembly and functional annotation

Clean, high quality reads were obtained by removing the adaptor sequences, reads with ambiguous "N" bases and reads with more than 10% Q<20 bases. At the same time, Q20, Q30 and GC-content was of the clean data were calculated. De novo assembly of the transcriptome was performed Trinity software [29] with default parameters and no reference sequences. Briefly, reads were assembled into contigs using an optimized k-mer length (25-mer) by the Inchworm program at the first step. The minimally overlapping contigs were clustered into connected components by the Chrysalis program, and then the transcripts were constructed by the Butterfly program. Finally, the transcripts were further clustered based on nucleotide sequence similarity, and the longest transcripts in each cluster was regarded as a unigene. For detection of transcription profiles in different tissues, clean reads from each library were initially assembled separately. To obtain a uniform transcriptome reference across the samples, all clean reads from twelve libraries were pooled together and de novo assembled to generate unigenes for assembly evaluation, gene annotation, and expression analysis. To identify putative functions of *L. japonica* unigenes, the unigenes were annotated with the NCBI non-redundant databases (NR), Pfam, Swiss-Prot, Gene Ontology (GO), Clusters of Orthologous Group (COG) and Kyoto Encyclopedia of Genes and Genomes (KEGG) databases using BLASTX searches (E-value $\leq 1.0e^{-5}$). The Blast2GO software package was used to compare and determine the unigene GO annotations [30]. Finally, WEGO2.0 was used to obtain the GO functional classifications of all annotated

unigenes [31]. Based on KEGG mapping, unigenes were assigned to multiple pathways using BLASTx, thereby retrieving KEGG Orthology (KO) information.

Analysis of differentially expressed genes (DEGs)

To calculate the amount of gene expression of each unigene, we used the abundance of reads derived from each locus to estimate gene expression and calculate transcripts per kilobase million (TPM) values with the program RSEM (RNA-Seq by Expectation Maximization) [32]. By pairwise comparisons of the different libraries, the DEGs were performed with EdgeR package based on the read counts for each gene at different libraries [33]. In addition, the false discovery rate (FDR) control method was used to identify the threshold of the P-value in the significance tests. Significance of DEGs was determined based on FDR<0.01 and fold change ≥2 (log2 Ratio≥1).

Validation by RT-qPCR

Twelve selected DEGs involved in flower timing, floral scent and flower color were determined by RT-qPCR. Total RNA was extracted using the same method as described above, and then the first strand cDNA was synthesized using the Superscript III First Strand cDNA Synthesis System (Invitrogen, USA) following the manufacture's protocol. The primers were designed with the Primer premier 5.0 software and synthesized by Sangon Biotech Co., Ltd. (Shanghai, China). *LjActin* was used as an internal standard. The relative expression levels of genes were calculated using the 2−ΔΔCt method. The qPCR was conducted using the LightCycler® 480 (Roche, Germany) with the SYBR Green real-time PCR Master Mix. Real-time quantification was performed in a reaction mix containing 2 ul cDNA, 0.2uM gene-specific forward and reverse primers, 1*SYBER Green master mix in a final 20 μl reaction. qPCR cycling conditions were for 40 cycles, of 15s at 95℃, 30s at the annealing temperature at 60 ℃, 30s at the extension at 72 ℃ with 5min at 72 ℃ for final extension.

Results

RNA-seq and de novo assembly yielded 195,850 unigenes

To deeply understand the molecular mechanism of flower development in *L. japonica*, twelve libraries were constructed and sequenced by using an Illumina HiSeq X Ten platform with 150 paired-end reads. After cleaning and quality checking, about 107.40 Gb total clean reads were obtained and each library produced no less than 6.76 Gb clean reads. Q30 percentage (percent of bases with sequencing error rate lower than 1‰) were 94.47%, 95.19%, 95.27%, 95.31%, 94.11%, 94.43%, 94.96%, 95.46%, 95.47%, 95.19%, 94.84% and 95.04% respectively (Table S1). Subsequently, de novo assembly generated 408409 transcripts and 195850 unigenes, with the N50 (covering 50% of all the nucleotide sequences of the largest unigene length) of 2099 nt and 1310 nt, respectively. In total, 91643 unigenes (46.79%) were between 201 and 400 nt; 35435 unigenes (27.20%) were between 401 and 800 nt; 18007 unigenes (9.19%) were between 801 and 1200 nt; 9403 unigenes (8.02%) were between 1201 and 2000 nt; 17231 unigenes (8.80%) were longer than 2000 nt (Table 1).

Functional annotation of *L. japonica* transcriptome

To validate and annotate the assembled unigenes, the 195850 unigenes were BLASTX searches (E value ≤$1.0e^{-5}$) against public protein databases. As a result, a total of 84657 (43.23%) unigenes were predicted to be coding sequence and 65332 (77.17%), 56610 (66.87%), 40282 (47.58%), 54154 (63.97%), 56184 (66.37%) and 36592 (43.22%) unigenes had homologous sequences respectively in NR, Swiss-Prot, pfam, STRING, GO and KEGG databases (Table 2). According to the NR annotation, 36.05% of the mapped sequences revealed similarities greater than 80%while 63.95% showed similarities ranging from 20% to 80% (Fig. 1a). The E value distribution was comparable with 51.47% of the mapped sequences showing high homology (<10^{-30}), whereas 48.53% of homologous sequences ranged between 10^{-5} and 10^{-30} (Fig. 1b). The top five species hits were *Vitis vinifera* (10.04%), *Daucus carota subsp. Sativus* (4.91%), *Hordeum vulgare subsp. Vulgare* (3.11%), *Coffea canephora* (2.95%) and *Sesamum indicum* (2.61%) (Fig. 1c). Based on the BLASTX results, a total of 56184 unigenes were assigned to GO terms, including three categories, i.e., molecular function, biological processes, and cellular component (Fig. 2). In biological process, metabolic process, signal transduction and reproductive process were top3 (Fig. 2a). We were able to annotate 31778 unigenes to 25 COG functional categories, among which the “general function prediction only” represented the largest category (3962 unigenes, 12.47%), followed by “Posttranslational modification, protein turnover, chaperones” (3241 unigenes, 10.20%), “Translation, ribosomal structure and biogenesis” (2560 unigenes, 8.06%), “Carbohydrate transport and metabolism” (2559 unigenes, 8.05%) (Fig. 2b). To obtain a better understanding of biological functions of the unigenes, the annotated sequences were also searched against the KEGG database. A total of 42649 unigenes were assigned to KEGG pathways. Among these pathways, “Biosynthesis of secondary metabolites (ko01110)” represented the largest group (5439, 12.75%), followed by “Carbon metabolism (ko01200)” (1829, 4.29%), “Ribosome (ko03010)” (1630, 3.82%), “Biosynthesis of amino acid (ko01230)” (1377, 3.23%) (Fig. 2c).

Transcriptome profiles of *L. japonica*

In order to understand the relationship between the transcriptome database, we used read count data to perform unsupervised principal component analysis (PCA) (Fig. S1a). Along the PC1 axis, we observed three clusters, including opened flower tissues (white flowers (WF) and yellow flowers (YF)) within the first group, floral buds (BD) and leaves (LF) as the other two groups. Along the PC2 axis, the opened flowers were further separated into two groups. Correlation analysis based on Pearson’s distance matrix using the entire transcriptome dataset were shown in Fig. S1b. The PCA analysis and correlation matrix showed a good correlation between the replicate sets for each of the four tissue samples. These results suggested that WF and YF showed the most similarity of transcriptomes, whereas LF showed the greatest difference to other tissues. These results also indicated that the presence of signature unigenes associated with and specific to each tissue.

Differential expressional genes (DEGs) analysis in different tissues

Following transcriptome assembly and annotation, DEGs analysis was carried out with a criteria of fold change ≥2 and FDR < 0.05 between different tissues. Substantial transcriptional differences were seen in the pairwise comparisons between different tissues (Fig. 3a). The number of DEGs was high in the vegetative tissue when compared to the reproductive tissues. In the LF, 2525, 4453, 4703 transcripts were up-regulated and 2790, 2816, 3059 transcripts were down-regulated compared to their expression in the BD, WF and YF respectively, which indicated a large shift in the transcriptional program. WF and YF had the smallest number of DEGs, with 437 up-regulated and 559 down-regulated. This result was consistent with the PCA and hierarchical correlation data that the opened flowers (WF and YF) showed the most similarity of transcriptomes (Fig. S1). To further investigate gene expression profiles, hierarchical clustering of all DEGs were performed as shown in Fig. 3b.

The enriched biological process GO terms of the DEGs were analyzed between different two samples. Although many of the enriched GO terms were common, a few were unique in different sets of genes. For example, the GO terms related to shoot axis formation, second shoot formation, floral organ development, fruit morphogenesis were enriched in LF vs. BD (Fig. S2a), regulation of seed dormancy process, positive regulation of mitotic cell cycle, positive regulation of seed germination, mitochondria RNA metabolic process, cellular response to cold in LF vs. WF (Fig. S2b), response to cytokine, regulation of response to red or far-red, regulation of mitotic metaphase/anaphase, photosynthetic electron transport in photosynthesis in LF vs. YF (Fig. S2c), terpenoid catabolic process, regulation of phosphate process, regulation of nucleocytoplasmic transport, regulation of G2/M transition of mitotic process in BD vs. WF (Fig. S2d), terpenoid transport, regulation of timing of meristematic phase, regulation of programmed cell death, isoprenoid transport in BD vs. YF (Fig. S2e), response to temperature stimulus, flavin adenine dinucleotide binding, gibberellic acid mediated signaling pathway, RNA export from nucleus in WF vs. YF (Fig. S2f) .

The flowering time pathway in *L. japonica*

In the model plant *Arabidopsis thaliana*, genes involved in flowering transition have been well characterized [34, 35]. In this study, 70 unigenes to flowering control pathway were assigned based upon sequence homology search and a detailed flowering regulatory network of *L. japonica* was constructed (Fig. 4a). These genes were grouped into various flowering control pathways, which include photoperiod pathway genes such as *PHYA*, *PHYB*, *PHYC*, *CRY, FLAVIN-BINDING KELCH REPEAT F-BOX1* (*FKF1*), *ZEITLUPE* (*ZTL*); autonomous pathway genes such as *FPA*, *FLOWERING LOCUS D* (*FLD*), *FY*, *FLOWERING LATE KH MOTIF* (*FLK*), *Luminidependens* (*LD*); circadian clock genes such as *CIRCADIAN CLOCK ASSOCIATED 1* (*CCA1*), *CONSTANS* (*CO*), *EARLY FLOWERING3* (*ELF3*), *LATE ELONGATED HYPOCOTYL* (*LHY*); vernalization pathway genes such as *VERNALIZATION 5* (*VRN5*), *FRILIKE 1* (*FRL1*), *FRIGIDA ESSENTIAL 1* (*FES1*); Gibberellin (GA) pathway genes such as *GIBBERELLIC ACIDINSENSITIVE* (*GAI*), *RGL*, *GID1*; flowering integrator genes such as *FLC*, *FT*, *AGL24*, *SOC1*, *SHORT VEGETATIVE PHASE* (*SVP*) and floral meristem identify genes *LEAFY* (*LFY*) and *AP1* etc. All these were identified in our *L. japonica* RNA-seq database and their expression level in different tissues was analyzed in Fig. 4b. The transcript levels of key genes of flowering pathway and floral molecular networks were further analyzed in flower

development by RT-qPCR (Fig. 4c). AGL24 is a dosage-dependent activator for flowering. The expression of *LjAGL24* mRNA was relatively high in LF, a drastic decrease in BD, and followed by gradually increase during flower development (Fig. 4b, 4c). *SOC1* also functions as a flowering promoter, together with *AGL24*, activating downstream targets [36]. *LjSOC1* had the lowest expression in BD and increased 4-fold during flower development (Fig. 4b, 4c). *AP1*, a MADS-box flower specific gene, is involved in flowering transition and flower development. The expression of *LjAP1* was only detected in the inflorescence (BD, WF and YF) but not in vegetative tissues (LF) (Fig. 4b, 4c), suggesting that the function of AP1 in the specification of floral meristem is conserved [37]. FLC acts as a repressor of flowering and is a convergence point for environmental and endogenous pathways that regulate flowering time. The expression of *LjFLC1* is much higher than that of *LjFLC2*, indicating that *LjFLC1* may play the dominant role in regulating flowering time. *LjFLC1* exhibited the similar expression profiles of *AtFLC* [38], which is the highest expression level in LF and a gradual decrease during the flower maturation (Fig. 4b, 4c). Except of *AGL24*, *SOC1*, *AP1* and *FLC1*, some other genes associated with flowering time show dynamic change during flower development, such as *PHYA, LFY*, *FT*, *SVP*, *GI, CCA1, TOC* and *ZTL* (Fig. 4b), reinforcing the studies that these genes form a complex network to regulate the flower transition.

The floral aromas pathway in *L. japonica*

The volatile organic components of *L. japonica* are often used in foods, cigarettes and cosmetics [39]. Most of the floral volatile compounds in *L. japonica* belonged to monoterpenes and sesquiterpenes, leading us to analyze the KEGG annotation results regarding the biosynthesis of terpenoid backbone. In this study, we identified 54 candidate genes involved in the MEP and MVA pathways (Fig. 5a). Most of them were highly expressed, which might indicate the terpenoid biosynthesis pathway is active and dynamic in *L. japonica*. DXS and AACT are the first enzymes of the MEP and MVA pathways, respectively. The expression of some *LjDXS* (Trinity_DN49357_c3_g1) and *LjAACT* (Trinity_DN49155_c0_g3) genes were very high (FRKM value>3000) in flowers, indicating their vital roles in terpene volatiles in *L. japonica*. Some of the most highly expressed genes centered on the MEP pathway, such as *DXS*, *HDS*, *IDS*, *GGPPS* (Fig. 5b), suggesting that this plastid pathway, might represent the major pathway for terpenoid biosynthesis in *L. japonica*. Within different tissues, MEP pathway genes, including *DXS*, *HDS*, *IDI*, *GGPPS* are relatively higher expressed in reproductive tissues than vegetative tissues, whereas genes involved in MVA pathway, such as *HMGS*, *HMGR*, *MVK*, and *MVD* were highest expressed in BD (Fig. 5b), at which the emission of volatile sesquiterpenoids has been shown to be high in *L. japonica*. To confirm the expression level of terpenoid-related genes in the MVA and MEP pathways, the expression of *MVK*, *MVD*, *HDS* and *IDS* genes at four tissues in *L. japonica* were tested by RT-qPCR. The results showed that the transcripts of *MVK* and *MVD* had the strongest expression in BD, whereas the transcript levels of *DXS* and *DXR* are relatively lower in leaves than in opened flowers (Fig. 5c). Eleven *TPS* unigenes were identified in the current transcriptome, including unigenes for monoterpenes linalool_synthase (*LIS*), α-terpineol synthase (*TPS-Cin*), geraniol synthase (*GES*), and sesquiterpenes (E)-nerolidol synthase (*NES*). The transcriptional patterns of *TPS* genes were very different in *L. japonica* (Fig. 5b), which was reasonable to explain the divergent volatile compound emissions in various tissues.

Genes related to flower color in *L. japonica*

Previous studies have shown that the content of chlorophyll and anthocyanin decreased dramatically during the early *L. japonica* flower development from the bud to the opened flowers, whereas the carotenoid went up substantially [24, 40]. Especially during the transformation from white flowers to yellow flowers, the content of carotenoid increased more than three times [40, 41]. In this study, we focused on the carotenoid and anthocyanin biosynthetic pathway in *L. japonica*. First, we identified 33 genes encoding enzymes involved in carotenoid biosynthetic pathway (Fig. 6a). PSY is the first and the rate-limiting enzyme in carotenoid skeleton production. We found that the level of *LjPSY* transcripts gradually increased during the developmental stage from BD to YF (Fig. 6b, 6c), which is consistent with the content of carotenoid in different developmental stages, indicating that *LjPSY* plays the vital role in carotenoid biosynthesis. Interestingly, the expression of some genes such as *LYCE* and *NSY* were decreased from BD to YF stage (Fig. 6b). Engineering of anthocyanin biosynthetic pathway in *L. japonica* is also detected. A total of 31 unigenes involved in anthocyanin biosynthetic pathway has been found to be expressed in *L. japonica* tissues (Fig. 6a). Some important enzymes were annotated more than 5 unigenes, such as *CHS*, *PAL*, *C4H*, *HCT*, *CYP73A* (Fig. 6a, 6b). The transcripts of *PAL*, *C4H*, *CHS*, *F3'H* showed the highest expression in LF, a dramatic decrease in BD and extremely low expression in the opened flowers. In contrast, the transcripts of *4CL*, *ANS*, *DFR* showed the highest expression in BD (Fig. 6b). To validate these data, the expression level of *PAL*, *PSY*, *CHS* and *ANS* were selected for RT-qPCR analysis. The relative expression level of these four genes were consistent with their relative abundances (Fig. 6c).

Real-time validation of RNA-seq data

To validate the results of the RNA-seq data, we performed real-time PCR to measure the expression levels of twelve floral trait relative genes at four tissues in *L. japonica*, including *LjAGL24* (Trinity_DN48871_c1_g2), *LjSOC1* (Trinity_DN49620_c0_g1), *LjAP1* (Trinity_DN47340_c3_g1), *LjFLC1* (Trinity_DN82380_c0_g1), *LjMVK* (Trinity_DN43630_c7_g4), *LjMVD* (Trinity_DN48885_c3_g1), *LjHDS* (Trinity_DN52168_c3_g2), *LjIDS* (Trinity_DN52586_c2_g4), *LjPSY* (Trinity_DN52905_c2_g3), *LjANS* (Trinity_DN41892_c1_g1), *LjPAL* (Trinity_DN50419_c0_g1) and *LjCHS* (Trinity_DN51090_c5_g2) (Table 3). Then we normalized and compared the real-time PCR results with that of RNA-Seq data. We found the gene expression levels measured by real-time PCR were highly consistent with that obtained from RNA-Seq analysis (Fig. 4c, 5c, 6c), suggesting the high quality of the transcriptome data.

Discussion

Sequencing and functional annotation

In our study, we sequenced twelve cDNA libraries from *L. japonica* leaves, floral buds, white flower and yellow flower with three biological replicates using the Illumina HiSeq X Ten platform, yielding 408409 transcripts and 195850 unigenes. Previous transcriptomic studies on *L. japonica* were mainly focused on

the biosynthesis of chlorogenic acid and luteolosides, the major two bioactive metabolites [3, 12, 42, 43], while the mechanism that control flower phenotypes of *L. japonica* is almost unknown. Our data focused on the expression of candidate genes involved in *L. japonica* floral transition and developmental processes. This result provided a genetic and molecular frame work for integrating different signaling pathways relevant to floral traits, contribution to the molecular breeding of the genus *Lonciera* and functional characterization of floral-related genes.

Genes related to the regulation of flowering time through five major pathways

L. japonica flowering is a highly coordinated, genetically programmed process by the interaction of floral transition genes, endogenous signals, and environmental factors. Previous studies have shown that the flowering time was controlled by five pathways in *Arabidopsis*, including photoperiod pathway, vernalization pathway, autonomous pathway, circadian clock pathway and GA pathway [15, 16]. In this study, the transcripts of *LjAGL24* and *LjSOC1* exhibit similar pattern with a relative high expression in LF, a drastic decrease in BD, and followed by a gradually increase during flower development (Fig. 4b, 4c). In *Arabidopsis*, *AGL24* and *SOC1* functions as flowering activators [36]. The reduction of AGL24 activity by RNAi results in late flowering, whereas overexpression of AGL24 causes precocious flowering [44]. *AGL24* mRNA is present in all of *Arabidopsis* tissues with the strongest expression in stem, a valley in flower bud and the gradually increased expression during flower development [44]. Similarly, *AtSOC1* was found to show a relatively high expression during vegetative stage, a downward trend to very low level during the transition to flowering, and a gradual increase during the flower development [38]. Our results show that the expression pattern of *LjAGL24* and *LjSOC1* are consistent with the previous studies of *AtAGL24* and *AtSOC1* [38, 45], indicating that *AGL24* and *SOC1* might play the essential and evolutionarily conserved roles in control of flowering switch across the plant kingdom. *AP1*, a MADS-box flower specific gene, is involved in flowering transition and flower development. The expression of *LjAP1* was only detected during the floral development but not in the vegetative tissues (Fig. 4b, 4c), similar to the expression of *AP1* in *Arabidopsis* and grapevine [37, 38], suggesting that the function of *AP1* in the specification of floral meristem is evolutionarily conserved. *FLC* is a key regulator of flowering time in *Arabidopsis*. The expression of *AtFLC* was high during the vegetative meristem development, maintained at low levels during the flowering transition, and continued the downward trend to a very low level during the flower development [38]. In the present study, the expression profiles of *LjFLC1* is similar to the expression profiles of *AtFLC*, suggesting its evolutionarily conserved roles in modulation of flowering time. Genes in the circadian clock/photoperiod pathway, play critical roles by regulating the expression of CO and floral integrator FT [46]. The mRNA level of *LjCO* and *LjFT* were at a low level (FPKM < 25), since we harvest the samples in the morning and these genes were accumulated in the evening [46]. In the present study, 70 candidate genes involved in flowering time pathway were identified (Fig. 4a) and their expression levels were analyzed (Fig. 4b), which enabled us to infer the regulatory network of flowering time genes in *L. japonica*. More detailed analyses of additional developmental stages or tissues would be beneficial for future investigations.

Volatile terpenoid metabolism genes in L. japonica

Terpenes, especially monoterpenes such as linalool, geraniol and nerol, but also some sesquiterpenes such as farnesene, nerolidol, and caryophyllene, are common constituents of floral scent in *L. japonica* [19]. The floral scent biosynthesis of terpenes have been studied in many plants, including *Syringa oblate* [47], *Salvia officinalis* [48], *Polianthes tuberosa* [49] and *Arabidopsis thaliana* [50]. The previous GC/MS analysis showed that the main volatile constituents of *L. japonica* are farnesol (16.2%) and linalool (11.0%) for the flower fraction, hexadecanoic acid (16.0%) and linalool (8.7%) for the leaf fraction, and hexadecanoic acid (31.4%) for the stems [19]. The regulation of terpenoid biosynthesis is complex, and the pathway fluxes are mostly controlled at the transcript level [51]. In this study, we identified 54 *L. japonica* genes encoding enzymes involved in terpenoid biosynthesis pathway. Our results showed that the genes involved in MVA pathway including *AACT*, *HMGCS*, *MVK*, and *MVD* had the strongest expression in floral buds, which was consistent with a strong emission of farnesol from these flower organs [19]. Moreover, our results support that farnesol is synthesized through MVA pathway as shown in Fig. 5a, and its biosynthesis and emission are closely correlated to the expression levels of those genes. Linalool was found to be an abundant volatile compound from *L. japonica* reproductive and vegetative tissues, accounting for 11.0% in flowers and 8.7% in leaves [19]. In this study, genes involved in the MEP pathway, such as *DXS*, *gcpE*, *ispS*, *GGPS* showed very high expression levels and broad expression patterns in four tissues (Fig. 5b), which may be attributable to the relatively high linalool contents in most *L. japonica* tissues.

The transcription regulation of carotenoid and anthocyanin biosynthetic pathways in L. japonica

During the process of *L. japonica* floral development, the flower color transits from the initial green to white and finally yellow in a short time frame. Metabolic analyses of pigment in *L. japonica* revealed that the content of chlorophyll and anthocyanin decreased drastically from bud to white flowers, whereas the carotenoid pigments went up substantially from white to yellow flowers [23, 24], suggesting that the early flower colors were mainly caused by the decreased level of anthocyanins and chlorophylls, and late flower color primarily by the increased contents of carotenoids [24]. There is increasing evidence that carotenogenesis in plant tissues is predominantly regulated at the transcriptional level [52]. For example, it was reported that a higher level of *PSY* and *DXS* might be responsible for the marigold color development from pale-yellow to orange [53]. In *Camellia nitidissima*, carotenoid synthesis pathway genes *PSY* and *crtZ* exert synergistic effects in carotenoid biosynthesis during flower development [54]. Previous studies showed that the expression level of *L. japonica PSY1*, *PDS1*, *PDS3* and *LCYB* were significantly higher during yellow flower stages than during early flower developmental stages [40]. In this study, 33 *L. japonica* unigenes were identified related to the carotenoid biosynthesis pathway. The mRNA level of *LjPSY* transcripts gradually increased during the developmental stage from floral bud to yellow flowers (Fig. 6c), which is consistent with previous reports [40]. In contrast, the expression of *LjLYCE* and *LjNSY* were decreased from BD to YF stage (Fig. 6b). These results can be plausibly explained by the fact that the amount of carotenoids in the tissues is not only attributed to the synthesis of carotenoids, but also to carotenoid degradation and sink capacity [55]. Indeed, the *L. japonica* genes encoding carotenoid cleavage dioxygenases (*LjCCD4* and *LjCCD1b*) exhibited stable expression during the flower development and played important roles in carotenoid degradation [40]. In *L. japonica*, the previous studies have

identified 11 DEGs involved in the anthocyanin biosynthetic pathway, and all of them were most highly expressed in the early flower development [24]. In this study, we identified 31 unigenes encoding 10 putative enzymes involved in anthocyanin biosynthesis. The transcript level of *PAL*, *C4H*, *CHS*, *F3'H* showed the highest expression in LF, while the transcripts of *4CL*, *ANS*, *DFR* showed the highest expression in BD. The expression level of most anthocyanin biosynthetic genes was dramatically decrease during the flower developmental stages (Fig. 6b), which is consistent with the sharp decline in the contents of anthocyanin from bud to the opened flowers.

Conclusion

In the present study, the complete transcriptome of *L. japonica* was de novo-assembled and annotated, generating a total of 195850 unigenes, of which 84657 could be functionally annotated. The candidate genes involved in flowering transition were identified and the flowering regulatory network of five pathways was constructed in *L. japonica*. The expression profiles of some floral integrator genes indicate that these key integrators might play the essential and evolutionarily conserved roles in control of flowering switch across the plant kingdom. We also identified 54 *L. japonica* genes encoding enzymes involved in terpenoid biosynthesis pathway. Most highly expressed genes centered on the MEP pathway, suggesting that this plastid pathway might represent the major pathway for terpenoid biosynthesis in *L. japonica*. In addition, the key genes involved in the carotenogenesis and anthocyanin biosynthesis pathway were identified, which may elucidate the regulatory mechanisms of flower color transitions in *L. japonica*. These results provide insights into the molecular mechanisms underlying the flowering time, floral scent and flower color, and will be useful for molecular breeding of *L. japonica*.

Abbreviations

4CL: 4-coumarate: coenzyme A ligase; AGL24: AGAMOUS-LIKE 24; AP1: APETALA1; ANS: Anthocyanidin synthase; BD: floral bud; CGA: Chlorogenic acid; CHI: Chalcone isomerase; CHR: Chalcone reductase; CHS: Chalcone synthase; COG: Clusters of Orthologous Group; COVID-19: coronavirus disease 2019; CRTISO: carotenoid isomerase; CYP450: cytochrome P450; DFR: dihydroflavonol 4-reductase; DGE: digital gene expression; DMAPP: dimethylallyl diphosphate; F3'5'H: flavonoid-3', 5'-hydroxylase; F3'H: flavonoid 3'-monooxygenase; F3H: flavanone 3-hydroxylase; FDR: False discovery rate; FLC: FLOWERING LOCUS C; FLS: flavonol synthesis; FPKM: Fragments Per Kilobase of transcript per Million mapped reads; FPPS: farnesyl diphosphate synthase ; FT: FLOWERING LOCUS T; FPP: farnesyl diphosphate; G3P: glyceraldehyde-3-phosphate; GO: Gene Ontology; GPP: geranyl diphosphate; HDS: 1-hydroxy-2-methyl-2-(E)-butenyl-4-diphosphate synthase; IPP: isopentenyl diphosphate; KEGG: Kyoto Encyclopedia of Genes and Genomes; KO: KEGG Orthology; L. japonica: Lonicera japonica Thunb.; LF: leaf; LIS: linalool_synthase; LYCB: lycopene β–cyclase; LYCE: lycopene ε-cyclase; MEP: 2-C-methyl-D-erythritol 4-phosphate; MVA: mevalonic acid; MVD: mevalonate diphosphate decarboxylase; MVK: mevalonate kinase; NES: (E)-nerolidol synthase; NR: The protein databases of Non-redundant; PAL: Phenylalanine ammonia-lyase; PCA: Principal component analysis; PDS: phytoene desaturase; PSY: phytoene synthase;

RNA-Seq: RNA sequencing; RSEM: RNA-Seq by Expectation Maximization; RT-qPCR: Real-time quantitative PCR; SARS-CoV-2: severe acute respiratory syndrome coronavirus 2; SOC1: SUPPRESSOR OF OVEREXPRESSION OF CONSTANS 1; TPS: terpene synthase; WF: white flower; YF: yellow flower; ZDS: ζ-carotene desaturase; Z-ISO: 15-cis-ζ-carotene isomerase

Declarations

Authors' contributions

LS and YS conceived and designed the experiments. LS and YC performed the experiments. LS and YC analyzed the data. LS and YS wrote the paper. All the authors have read and approved the final version of the manuscript.

Ethics declarations

Ethics approval and consent to participate

All the plant materials used in this study were provided by Fengqiu cultivation base, Henan province, China. The experiments were conducted under local legislation and permissions.

Availability of data and materials

All the data generated or analysed during this study are included in this published article and its supplementary information files. The datasets used and/or analysed during the current study are available from the corresponding author (s.y0001@163.com) on reasonable request.

Consent for publication

Not applicable.

Competing interests

The authors declare that they have no competing interests.

Plant Ethics – Permission

Lonicera japonica materials used in this study were collected from Fengqiu cultivation base (35°05'N and 114°25'E), Henan province, China. The permissions were obtained from Fengqiu country Xinfeng honeysuckle planting cooperatives.

Plant Guidelines

Experimental research and field studies on *Lonicera japonica* in this study is complied with relevant institutional, national, and international guidelines and legislation.

References

1. Schierenbeck KA: **Japanese honeysuckle (Lonicera japonica) as an invasive species; history, ecology, and context**. *Critical Reviews in Plant Sciences* 2004, **23**(5):391–400.
2. Shang X, Pan H, Li M, Miao X, Ding H: **Lonicera japonica Thunb.: ethnopharmacology, phytochemistry and pharmacology of an important traditional Chinese medicine**. *Journal of Ethnopharmacology* 2011, **138**(1):1–21.
3. Yuan Y, Song L, Li M, Liu G, Chu Y, Ma L, Zhou Y, Wang X, Gao W, Qin S *et al*: **Genetic variation and metabolic pathway intricacy govern the active compound content and quality of the Chinese medicinal plant Lonicera japonica thunb**. *BMC Genomics* 2012, **13**:195.
4. Kwak WJ, Cho YB, Han CK, Shin HJ, Ryu KH, Yoo H, Rhee HI: **Extration and purification method of active constituents from stem of Lonicera japonica thunb., its usage for anti-inflammatory and analgesic drug**. *Australian Patent* EP; 2005.
5. Lin L, Wang P, Du Z, Wang W, Cong Q, Zheng C, Jin C, Ding K, Shao C: **Structural elucidation of a pectin from flowers of Lonicera japonica and its antipancreatic cancer activity**. *Int J Biol Macromol* 2016, **88**:130–137.
6. Jahan I, Onay A: **Potentials of plant-based substance to inhabit and probable cure for the COVID-19**. *Turk J Biol* 2020, **44**(3):228–241.
7. Yang Y, Islam MS, Wang J, Li Y, Chen X: **Traditional chinese medicine in the treatment of patients infected with 2019-new coronavirus (SARS-CoV-2): A review and perspective**. *Int J Biol Sci* 2020, **16**(10):1708–1717.
8. Hu K, Guan WJ, Bi Y, Zhang W, Li L, Zhang B, Liu Q, Song Y, Li X, Duan Z *et al*: **Efficacy and safety of Lianhuaqingwen capsules, a repurposed Chinese herb, in patients with coronavirus disease 2019: A multicenter, prospective, randomized controlled trial**. *Phytomedicine* 2020:153242.
9. Zhou LK, Zhou Z, Jiang XM, Zheng Y, Chen X, Fu Z, Xiao G, Zhang CY, Zhang LK, Yi Y: **Absorbed plant MIR2911 in honeysuckle decoction inhibits SARS-CoV-2 replication and accelerates the negative conversion of infected patients**. *Cell Discov* 2020, **6**:54.
10. Wang H, Li Y, Wang S, Kong D, Sahu SK, Bai M, Li H, Li L, Xu Y, Liang H *et al*: **Comparative transcriptomic analyses of chlorogenic acid and luteolosides biosynthesis pathways at different flowering stages of diploid and tetraploid Lonicera japonica**. *PeerJ* 2020, **8**:e8690.
11. Yang B, Zhong Z, Wang T, Ou Y, Tian J, Komatsu S, Zhang L: **Integrative omics of Lonicera japonica Thunb. Flower development unravels molecular changes regulating secondary metabolites**. *J Proteomics* 2019, **208**:103470.
12. He L, Xu X, Li Y, Li C, Zhu Y, Yan H, Sun Z, Sun C, Song J, Bi Y *et al*: **Transcriptome analysis of buds and leaves using 454 pyrosequencing to discover genes associated with the biosynthesis of active ingredients in Lonicera japonica Thunb**. *PLoS One* 2013, **8**(4):e62922.
13. O'Maoileidigh DS, Graciet E, Wellmer F: **Gene networks controlling Arabidopsis thaliana flower development**. *New Phytol* 2014, **201**(1):16–30.

14. Huang M, Sanchez-Moreiras AM, Abel C, Sohrabi R, Lee S, Gershenzon J, Tholl D: **The major volatile organic compound emitted from Arabidopsis thaliana flowers, the sesquiterpene (E)-beta-caryophyllene, is a defense against a bacterial pathogen**. *New Phytol* 2012, **193**(4):997–1008.
15. Bouche F, Lobet G, Tocquin P, Perilleux C: **FLOR-ID: an interactive database of flowering-time gene networks in Arabidopsis thaliana**. *Nucleic Acids Res* 2016, **44**(D1):D1167-1171.
16. Mouradov A, Cremer F, Coupland G: **Control of flowering time: interacting pathways as a basis for diversity**. *Plant Cell* 2002, **14 Suppl**:S111-130.
17. Blumel M, Dally N, Jung C: **Flowering time regulation in crops-what did we learn from Arabidopsis?** *Curr Opin Biotechnol* 2015, **32**:121–129.
18. Albani MC, Coupland G: **Comparative analysis of flowering in annual and perennial plants**. *Curr Top Dev Biol* 2010, **91**:323–348.
19. Vukovic N, Kacaniova M, Hleba L, Sukdolak S: **Chemical composition of the essential oils from the flower, leaf and stem of Lonicera japonica**. *Nat Prod Commun* 2012, **7**(5):641–644.
20. Muhlemann JK, Klempien A, Dudareva N: **Floral volatiles: from biosynthesis to function**. *Plant Cell & Environment* 2014, **37**(8).
21. Weitzel C, Simonsen HT: **Cytochrome P450-enzymes involved in the biosynthesis of mono- and sesquiterpenes**. *Phytochemistry Reviews* 2013.
22. Boachon B, Junker RR, Miesch L, Bassard JE, Hofer R, Caillieaudeaux R, Seidel DE, Lesot A, Heinrich C, Ginglinger JF *et al*: **CYP76C1 (Cytochrome P450)-mediated linalool metabolism and the formation of volatile and soluble linalool oxides in Arabidopsis flowers: A strategy for defense againstfloral antagonists**. *Plant Cell* 2015, **27**(10):2972–2990.
23. Fu L, Li H, Li L, Yu H, Wang L, Aamp N, University F: **Reason of flower color change in Lonicera japonica**. *Scientia Silvae Sinicae* 2013.
24. Xue Q, Fan H, Yao F, Cao X, Liu M, Sun J, Liu Y: **Transcriptomics and targeted metabolomics profilings for elucidation of pigmentation in Lonicera japonica flowers at different developmental stages**. *Industrial Crops and Products* 2020, **145**:111981.
25. Tanaka Y, Sasaki N, Ohmiya A: **Biosynthesis of plant pigments: anthocyanins, betalains and carotenoids**; 2008.
26. Cazzonelli CI, Pogson BJ: **Source to sink: regulation of carotenoid biosynthesis in plants**. *Trends in Plant Science* 2010, **15**(5):266–274.
27. Fang H, Qi X, Li Y, Yu X, Xu D, Liang C, Li W, Liu X: **De novo transcriptomic analysis of light-induced flavonoid pathway, transcription factors in the flower buds of Lonicera japonica**. *Trees (Berl West)* 2020, **34**(1):267–283.
28. Qi X, Yu X, Xu D, Fang H, Dong K, Li W, Liang C: **Identification and analysis of CYP450 genes from transcriptome of Lonicera japonica and expression analysis of chlorogenic acid biosynthesis related CYP450s**. *PeerJ* 2017, **5**:e3781.

29. Grabherr MG, Haas BJ, Yassour M, Levin JZ, Thompson DA, Amit I, Adiconis X, Fan L, Raychowdhury R, Zeng Q *et al*: **Full-length transcriptome assembly from RNA-Seq data without a reference genome**. *Nature Biotechnology* 2011, **29**(7):644–652.
30. Conesa A, Gotz S, Garcia-Gomez JM, Terol J, Talon M, Robles M: **Blast2GO: a universal tool for annotation, visualization and analysis in functional genomics research**. *Bioinformatics* 2005, **21**(18):3674–3676.
31. Ye J, Zhang Y, Cui H, Liu J, Wu Y, Cheng Y, Xu H, Huang X, Li S, Zhou A *et al*: **WEGO 2.0: a web tool for analyzing and plotting GO annotations, 2018 update**. *Nucleic Acids Res* 2018, **46**(W1):W71-W75.
32. Li B, Dewey CN: **RSEM: accurate transcript quantification from RNA-Seq data with or without a reference genome**. *BMC Bioinformatics* 2011, **12**:323.
33. Robinson MD, McCarthy DJ, Smyth GK: **edgeR: a Bioconductor package for differential expression analysis of digital gene expression data**. *Bioinformatics* 2009, **26**(1):139–140.
34. Fornara F, de Montaigu A, Coupland G: **SnapShot: Control of flowering in Arabidopsis**. *Cell* 2010, **141**(3):550, 550 e551-552.
35. Khan MR, Ai XY, Zhang JZ: **Genetic regulation of flowering time in annual and perennial plants**. *Wiley Interdiscip Rev RNA* 2014, **5**(3):347–359.
36. Immink RG, Pose D, Ferrario S, Ott F, Kaufmann K, Valentim FL, de Folter S, van der Wal F, van Dijk AD, Schmid M *et al*: **Characterization of SOC1's central role in flowering by the identification of its upstream and downstream regulators**. *Plant Physiol* 2012, **160**(1):433–449.
37. Zhang N, Wen J, Zimmer EA: **Expression patterns of AP1, FUL, FT and LEAFY orthologs in Vitaceae support the homology of tendrils and inflorescences throughout the grape family**. *Journal of Systematics and Evolution* 2015, **53**(5):469–476.
38. Klepikova AV, Logacheva MD, Dmitriev SE, Penin AA: **RNA-seq analysis of an apical meristem time series reveals a critical point in Arabidopsis thaliana flower initiation**. *BMC Genomics* 2015, **16**:466.
39. Rahman A, Kang SC: **In vitro control of food-borne and food spoilage bacteria by essential oil and ethanol extracts of Lonicera japonica Thunb**. *Food Chemistry* 2009, **116**(3):670–675.
40. Pu X, Li Z, Tian Y, Gao R, Hao L, Hu Y, He C, Sun W, Xu M, Peters RJ *et al*: **The honeysuckle genome provides insight into the molecular mechanism of carotenoid metabolism underlying dynamic flower coloration**. *New Phytol* 2020, **227**(3):930–943.
41. Li J, Lian X, Ye C, Wang L: **Analysis of Flower Color Variations at Different Developmental Stages in Two Honeysuckle (Lonicera Japonica Thunb.) Cultivars**. *HortScience* 2019, **54**:779–782.
42. Rai A, Kamochi H, Suzuki H, Nakamura M, Takahashi H, Hatada T, Saito K, Yamazaki M: **De novo transcriptome assembly and characterization of nine tissues of Lonicera japonica to identify potential candidate genes involved in chlorogenic acid, luteolosides, and secoiridoid biosynthesis pathways**. *J Nat Med* 2017, **71**(1):1–15.
43. Wang H, Li Y, Wang S, Kong D, Sahu SK, Bai M, Li H, Li L, Xu Y, Liang H *et al*: **Comparative transcriptomic analyses of chlorogenic acid and luteolosides biosynthesis pathways at different flowering stages of diploid and tetraploid Lonicera japonica**. *PeerJ* 2020, **8**:e8690-e8690.

44. Yu H, Xu Y, Tan EL, Kumar PP: **AGAMOUS-LIKE 24, a dosage-dependent mediator of the flowering signals**. *Proc Natl Acad Sci U S A* 2002, **99**(25):16336–16341.
45. Samach A, Onouchi H, Gold SE, Ditta GS, Schwarz-Sommer Z, Yanofsky MF, Coupland G: **Distinct roles of CONSTANS target genes in reproductive development of Arabidopsis**. *Science* 2000, **288**(5471):1613–1616.
46. Imaizumi T: **Arabidopsis circadian clock and photoperiodism: time to think about location**. *Curr Opin Plant Biol* 2010, **13**(1):83–89.
47. Zheng J, Hu Z, Guan X, Dou D, Bai G, Wang Y, Guo Y, Li W, Leng P: **Transcriptome analysis of Syringa oblata Lindl. inflorescence identifies genes associated with pigment biosynthesis and scent metabolism**. *PLoS One* 2015, **10**(11):e0142542.
48. Ali M, Li P, She G, Chen D, Wan X, Zhao J: **Transcriptome and metabolite analyses reveal the complex metabolic genes involved in volatile terpenoid biosynthesis in garden sage (Salvia officinalis)**. *Scientific Reports* 2017, **7**(1).
49. Fan R, Chen Y, Ye X, Wu J, Lin B, Zhong H: **Transcriptome analysis of Polianthes tuberosa during floral scent formation**. *PLoS One* 2018, **13**(9):e0199261.
50. Chen F, Tholl D, D'Auria JC, Farooq A, Pichersky E, Gershenzon J: **Biosynthesis and emission of terpenoid volatiles from Arabidopsis flowers**. *Plant Cell* 2003, **15**(2):481–494.
51. Vranova E, Coman D, Gruissem W: **Network analysis of the MVA and MEP pathways for isoprenoid synthesis**. *Annu Rev Plant Biol* 2013, **64**:665–700.
52. Sandmann G, Rmer S, Fraser PD: **Understanding carotenoid metabolism as a necessity for genetic engineering of crop plants**. *Metabolic Engineering* 2006, **8**(4):291–302.
53. Moehs CP, Tian L, Osteryoung KW, Dellapenna D: **Analysis of carotenoid biosynthetic gene expression during marigold petal development**. *Plant Molecular Biology* 2001, **45**(3):281–293.
54. Zhou X, Li J, Zhu Y, Ni S, Chen J, Feng X, Zhang Y, Li S, Zhu H, Wen Y: **De novo Assembly of the Camellia nitidissima Transcriptome reveals key genes of flower pigment biosynthesis**. *Front Plant Sci* 2017, **8**:1545.
55. Tanaka Y, Sasaki N, Ohmiya A: **Biosynthesis of plant pigments: anthocyanins, betalains and carotenoids**. *Plant J* 2008, **54**(4):733–749.

Tables

Due to technical limitations, the tables are only available as a download in the supplemental files section.

Figures

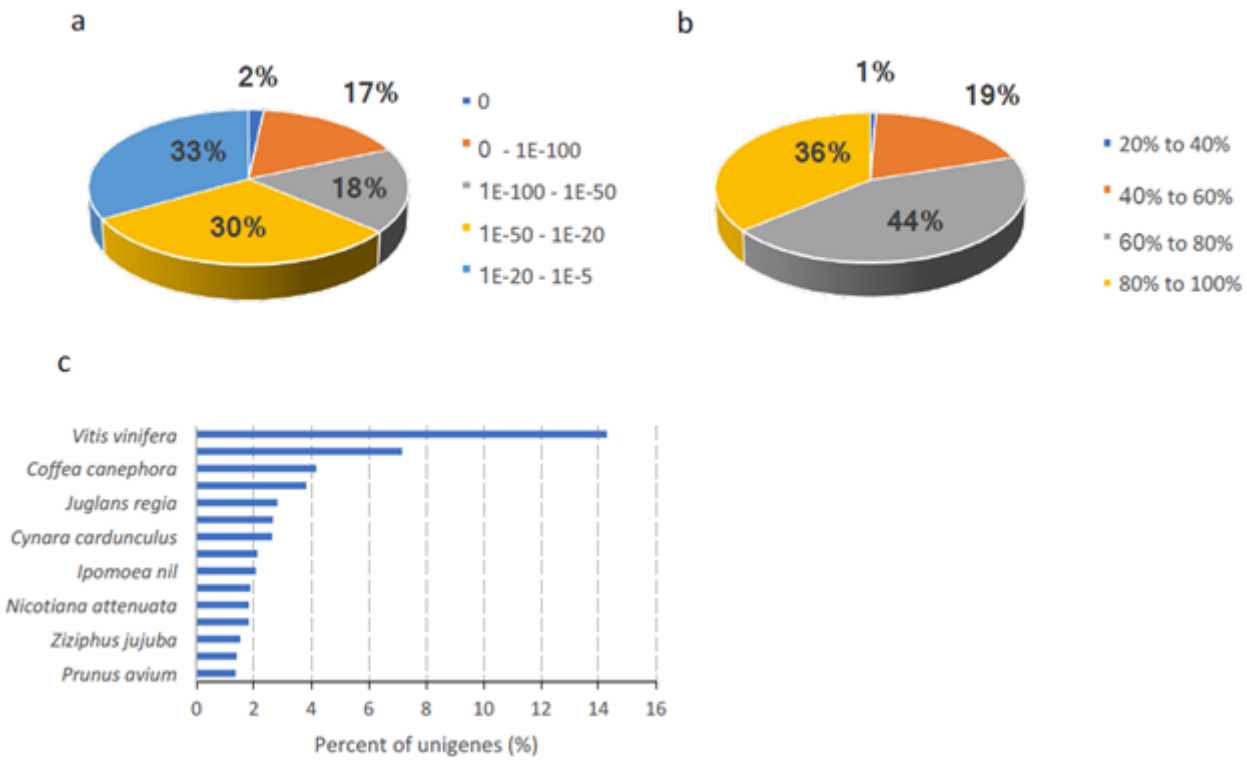

Figure 1

Results of a similarity search of the assembled sequences against the Nr database. (a) E-value distribution of blast hits for each unique sequence with E value ≤10-5. (b) Similarity distribution of the top blast hits for each sequence. (c) BLAST Top-Hits species distribution when compared with NR database.

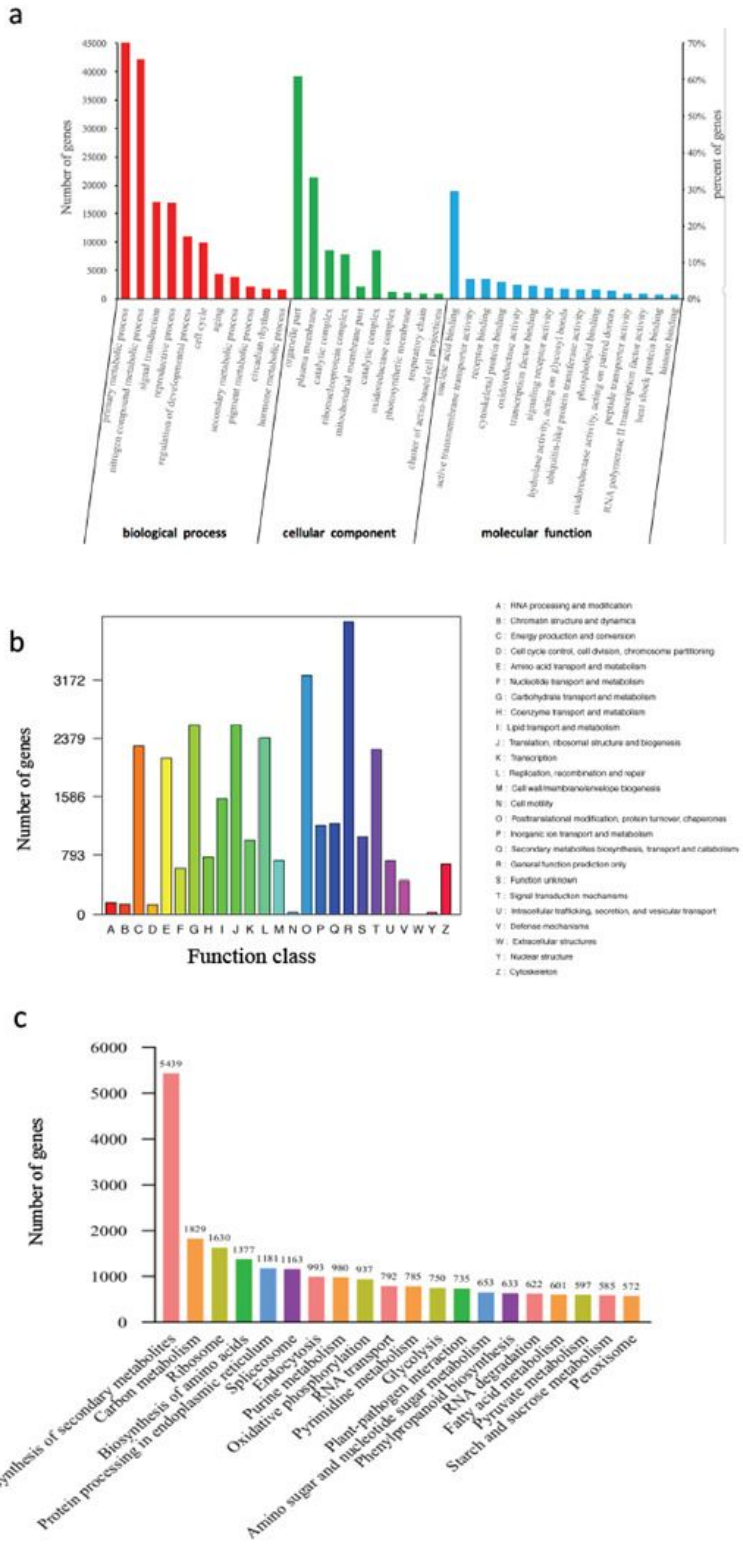

Figure 2

Analysis of functional categories of annotated unigenes in L. japonica. (a) Gene ontology classification of annotated unigenes. (b) KOG functional classification of all unigene sequences. (c) KEGG classfication of assembled unigenes.

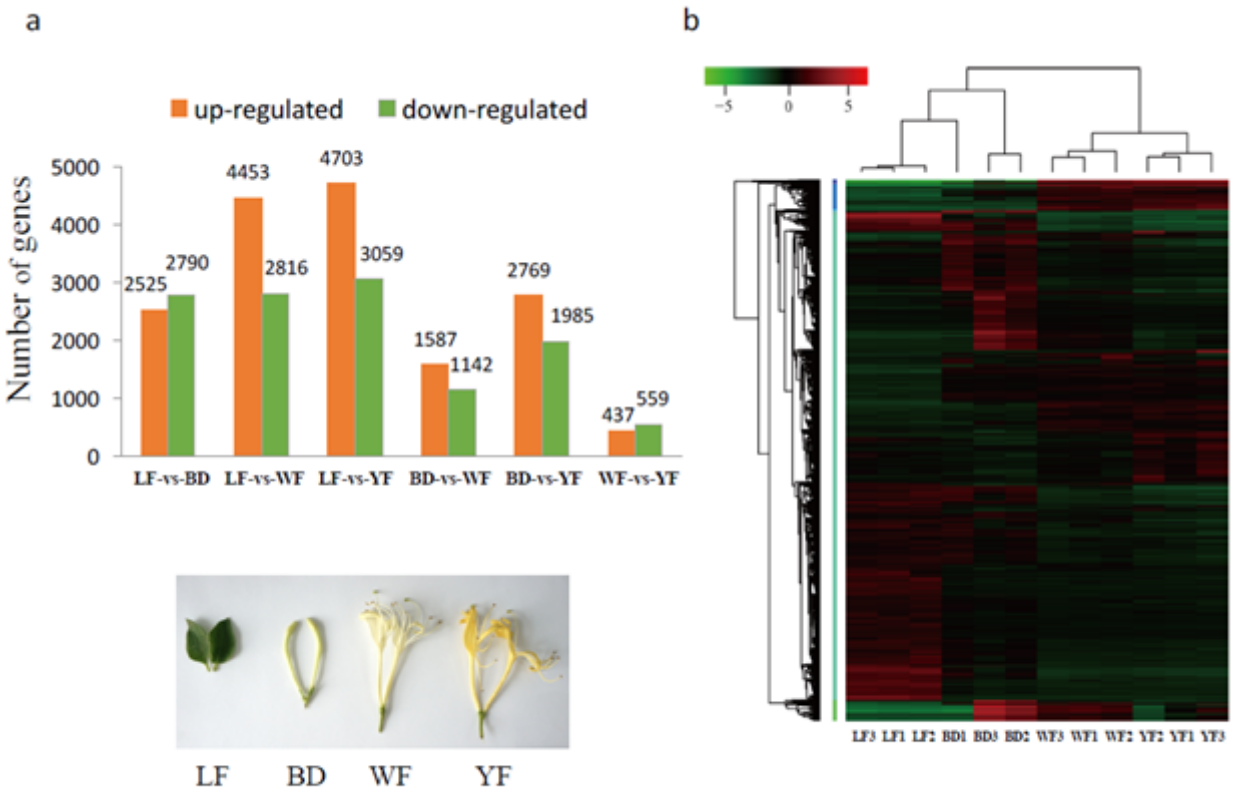

Figure 3

Analysis of DEGs in L. japonica different tissues. (a) Number of DEGs in the six pair-wise comparisons. (b) Hierarchical clustering of all DEGs in L. japonica different tissues.

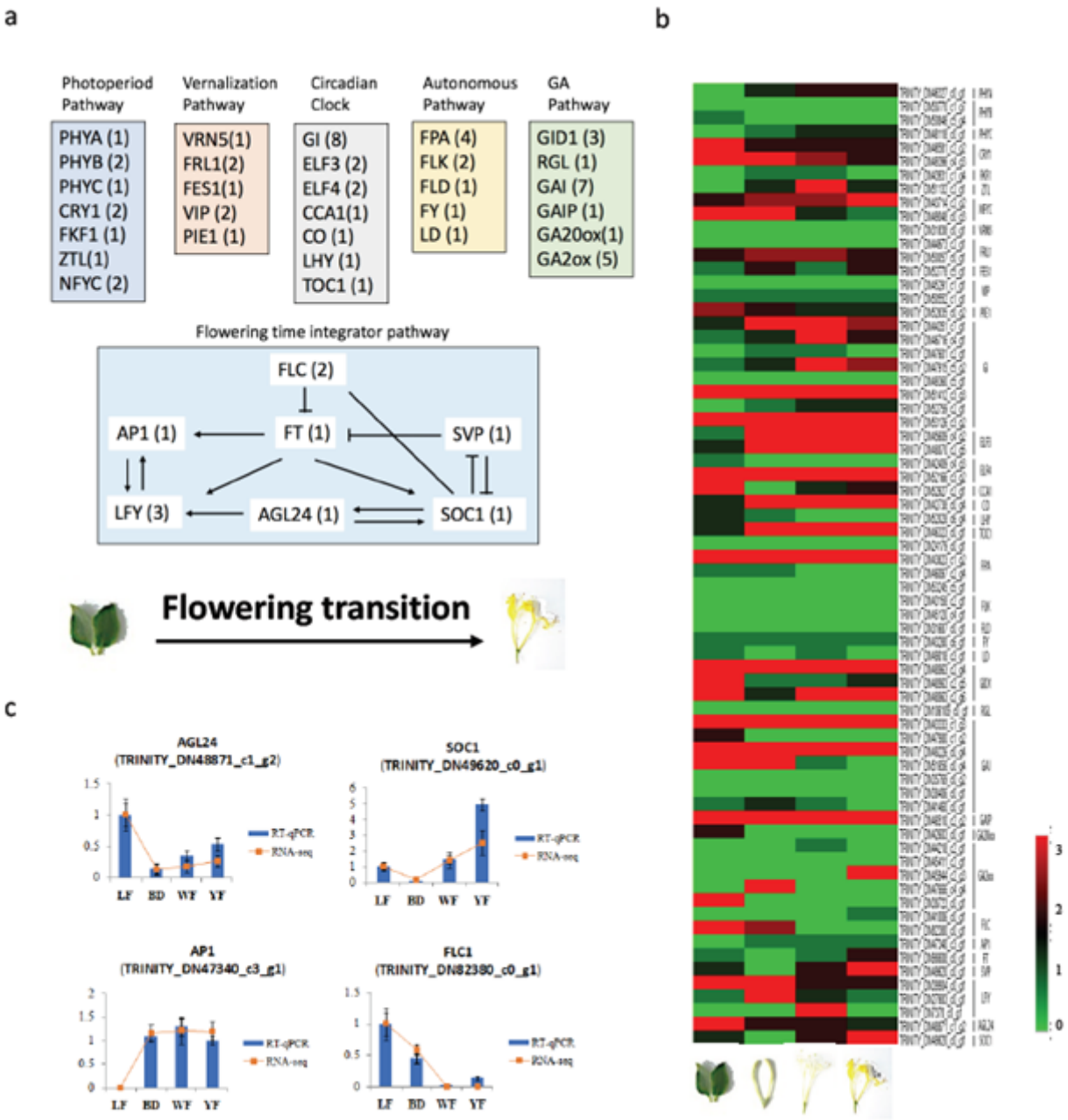

Figure 4

The flowering time pathway in L. japonica. (a) Simplified model of the main regulatory genes and flowering pathway acting in L. japonica. (b) Heatmap of the expressed genes assigned to flowering time pathway. Red and green indicate up- and down-regulated transcripts , respectively. (c) Real-time PCR analysis of AGL24, SOC1, AP1 and FLC1 genes during the LF stage, BD stage, WF stage and YF stage of L. japonica. The y-axis indicates fold change in expression among the samples. Expression levels were normalized using LjActin genes. Error bars indicate the standard deviation of the mean (SD) (n=3).

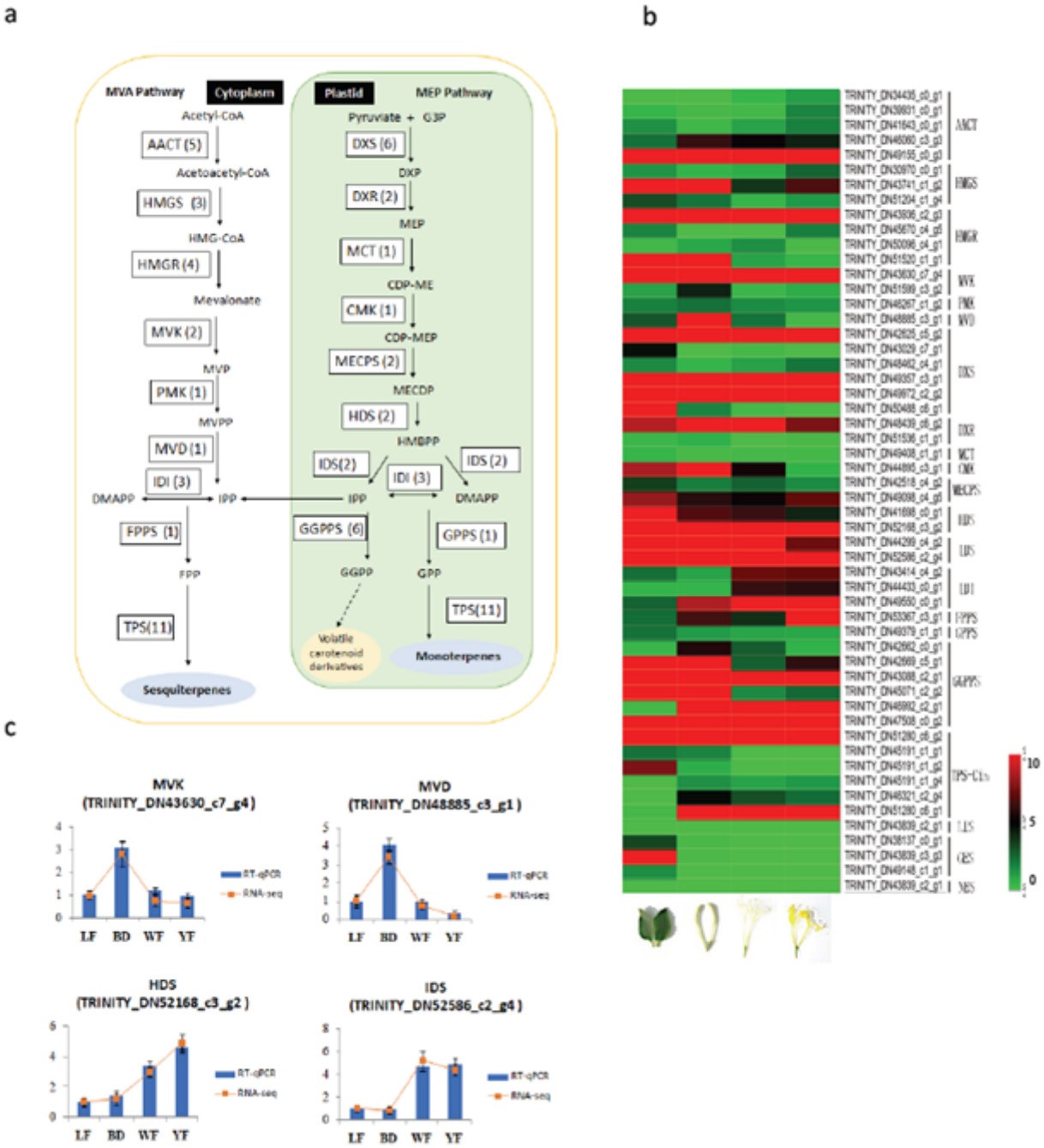

Figure 5

The terpenoid biosynthesis pathways in L. japonica. (a) The representative terpenoid biosynthetic pathways from L. japonica transcriptome data with substrates and products. (b) Heatmap for the transrcipt levels of genes assigned to the terpenoid biosynthesis pathway. Red and green indicate up- and down-regulated transcripts , respectively. (c) The expression levels and patterns of MVK, MVD, HDS and IDS were confirmed by qRT-PCR during the LF stage, BD stage, WF stage and YF stage of L. japonica. . Expression levels were normalized using LjActin genes. Error bars represent the SD of the mean values (n=3).

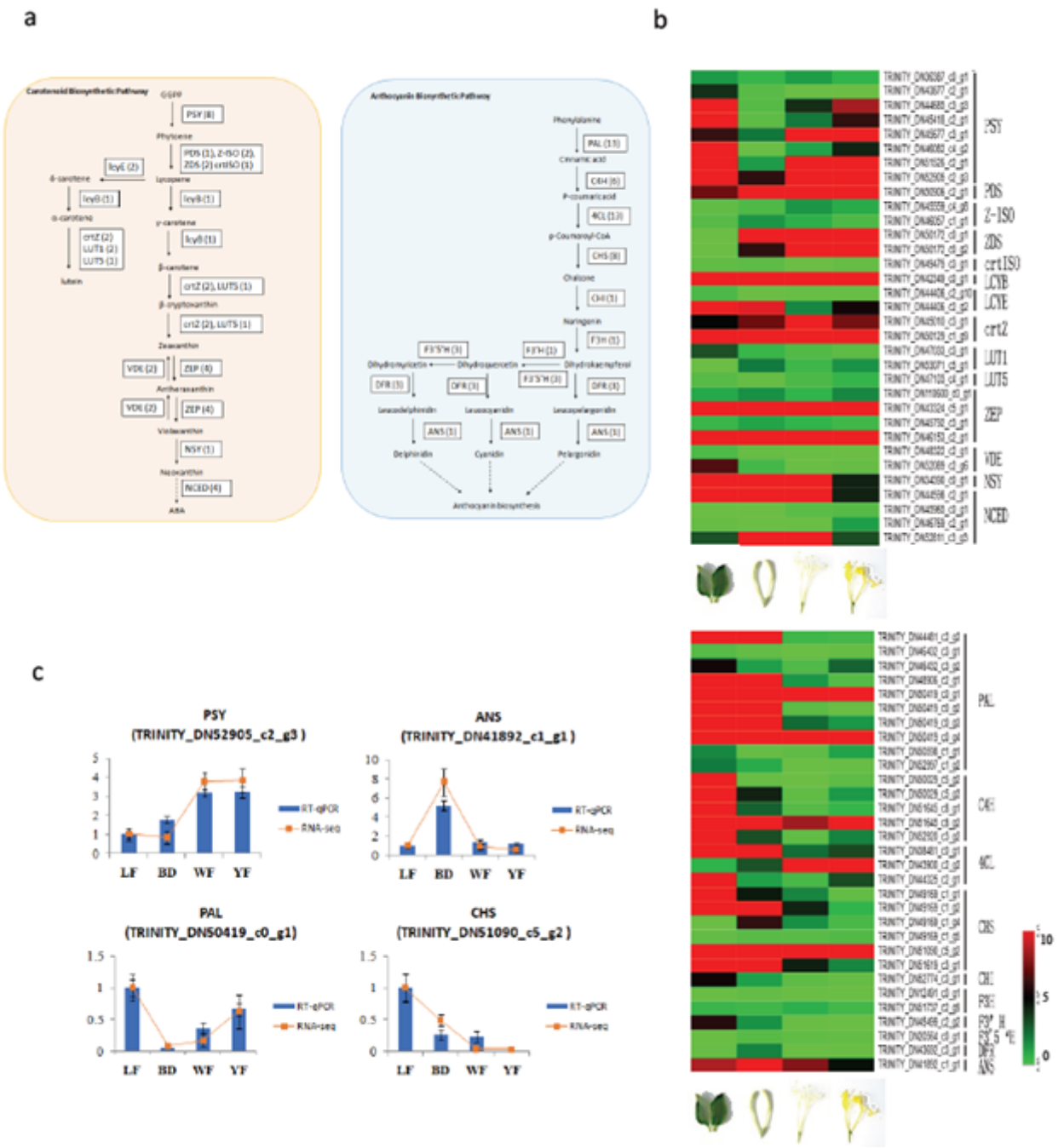

Figure 6

The carotenoid and anthocyanin biosynthesis pathways in L. japonica. (a) The representative carotenoid and anthocyanin biosynthetic pathways from L. japonica transcriptome data with substrates and products. (b) Heatmap for the transcript levels of genes assigned to the carotenoid and anthocyanin biosynthesis pathway. Red and green indicate high-expression and low-expression, respectively. (c) The expression levels and patterns of PSY, ANS, PAL and CHS of were confirmed by qRT-PCR during the LF stage, BD stage, WF stage and YF stage of L. japonica. Expression levels were normalized using LjActin genes. Error bars represent the SD of the mean values (n=3).

Supplementary Files

This is a list of supplementary files associated with this preprint. Click to download.

- TablesJan232021.pdf
- supplementalFeb20Lj.pdf